JACS
JOURNAL OF THE AMERICAN CHEMICAL SOCIETY
Communication
pubs.acs.org/JACS

Dihydrogen Trioxide (HOOOH) Photoelimination from a Platinum(IV) Hydroperoxo-Hydroxo Complex

Lasantha A. Wickramasinghe and Paul R. Sharp*

Department of Chemistry, University of Missouri, 125 Chemistry Building, Columbia, Missouri 65211-7600, United States

Supporting Information

ABSTRACT: Photolysis (380 nm) of *trans*-Pt(PEt$_3$)$_2$(Cl)(OH)(OOH)(4-trifluoromethylphenyl) (**1**) at −78 °C in acetone-d_6 or toluene-d_8 yields HOOOH (16−20%) and *trans*-Pt(PEt$_3$)$_2$(Cl)(4-trifluoromethylphenyl) (**2**). Also observed in acetone-d_6 are H_2O_2, $(CD_3)_2C(OH)(OOH)$, and $(CD_3)_2C(OOH)_2$. Thermal decomposition or room-temperature photolysis of **1** gives O_2, water, and **2**. Computational modeling (DFT) suggests two intramolecular hydrogen-bonding-dependent triplet pathways for the photolysis and two possible pathways for the thermolysis, one involving proton transfer from the OOH to the OH ligand and the other homolysis of the Pt−OOH bond, abstraction of the OH ligand, and decomposition of the resulting H_2O_3. Trapping studies suggest the latter pathway.

We recently reported the first synthesis of the Pt(IV) hydroxo-hydroperoxo complex *trans*-Pt(PEt$_3$)$_2$(Cl)(OH)(OOH)(4-tft) (**1**) (4-tft = 4-trifluoromethylphenyl) by oxidation of the Pt(II) complex *trans*-Pt(PEt$_3$)$_2$(Cl)(4-tft) (**2**) with H_2O_2.[1] We now report the thermal and photochemistry of **1**, which includes reductive elimination of HOOOH (H_2O_3, dihydrogen trioxide or trioxidane), a rare example of O−O bond formation by photoreductive elimination. (Other examples feature H_2O_2 elimination.[2−6]). We extend our discussion with computational modeling studies on the thermodynamics and mechanisms for these unusual reactions.

Although the existence of H_2O_3 has been proposed for many years, its solution synthesis, identification, and characterization are relatively recent.[7] Laboratory synthetic procedures involve the hydrogenation of ozone with various reagents,[8] including H_2O_2, where the mixture is known as a powerful oxidizing system (peroxone process).[9] H_2O_3 has also been proposed to form in an antibody-catalyzed reaction of singlet oxygen with water.[10,11] It is unstable in solution at room temperature, decomposing to water and singlet oxygen, but it is stable in organic solvents at low temperatures (−60 °C). It can be readily detected by its distinctive ^{1}H NMR chemical shift (δ 13.4 in acetone-d_6).[8] The chemistry below describes a novel method for H_2O_3 formation by coupling of an OOH ligand and an OH ligand.

Irradiation (380 nm) of **1** at ambient temperature for ∼8 min in C_6D_6 results in reduction of the Pt center, yielding the Pt(II) complex **2**, water, and presumably O_2 (eq 1). This observation caught our attention, as there are at least two possible pathways to water and O_2. One would be directly through photodriven abstraction of a hydrogen atom from the OOH ligand by OH.

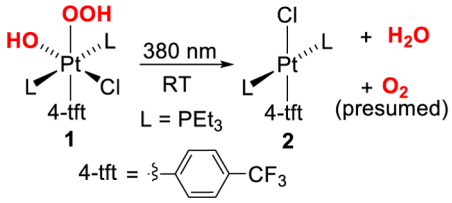

eq 1

(We initially considered this to be the more likely pathway.) The other would be by decomposition of H_2O_3, the expected photoreductive elimination product if the photochemistry of **1** follows that of the analogous hydroxo-halo complexes *trans*-Pt(PEt$_3$)$_2$(Cl)(OH)(X)(4-tft) (X = Cl, Br)[1] and bromo complexes *trans*-Pt(PEt$_3$)$_2$(Br)$_3$R.[12] With these possibilities in mind, the photolysis of **1** was reexamined at −78 °C.

An acetone-d_6 sample of **1** in an NMR tube was cooled to −78 °C and irradiated at 380 nm. ^{1}H NMR analysis was then carried out at −60 °C and revealed a singlet at δ 13.4 that reached a maximum at 40−60% conversion of **1** into **2** and then declined and disappeared as the irradiation continued. The peak also disappeared when the sample was warmed to RT. The experiment was repeated in toluene-d_8, where H_2O_3 gives a singlet at δ 9.9.[8] A singlet at this chemical shift was observed at −60 °C, confirming the formation of H_2O_3 from the photolysis of **1** (eq 2). ^{1}H NMR spectral integration indicated H_2O_3 yields[13]

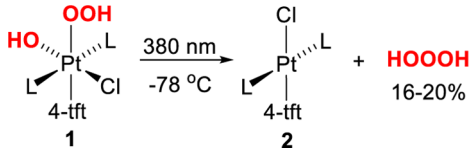

eq 2

of 16 ± 2% in toluene-d_8 and 6 ± 2% in acetone-d_6 at 40−60% conversion of **1**. However, it was noticed that the OOH signal of **1** was considerably diminished (by 70%) in acetone-d_6 and that a signal for HOD was present. We interpret this as a result of deuterium exchange of the OH and OOH ligands with residual D_2O from the acetone-d_6 preparation.[14,15] Correcting for this exchange increased the H_2O_3 yield in acetone-d_6 to 20%, similar to that in toluene-d_8.

Also detected in the low-temperature acetone-d_6 sample were ^{1}H NMR peaks in the δ 9−12 region attributed to H_2O_2 (9%) and acetone adducts **3** (16%) and **4** (36%), giving a total product yield of 81%. (Yields[13] include adjustment for H/D exchange.) Acetone adducts **3** and **4** are known to form in reactions of H_2O_2

Received: July 17, 2014
Published: September 19, 2014

   dx.doi.org/10.1021/ja507263f | J. Am. Chem. Soc. 2014, 136, 13979−13982

with acetone.[16−18] (Adduct **4** could also form by net addition of OOH and OH from **1** across the acetone double bond. We have observed similar photoreactions of alkenes with halogen analogues of **1**.[19]) No high-shift peaks, other than that of H_2O_3, are observed in the toluene-d_8 samples, but the H_2O_2 ^{1}H NMR signal is in the aromatic region and is broad, making it difficult to observe in toluene-d_8.

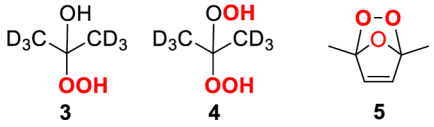

Room-temperature photolysis of **1** was also conducted in the presence of the singlet oxygen traps 2,5-dimethylfuran (DF) and 2,3-dimethyl-2-butene (TME). The DF singlet oxygen trapping product, endoperoxide **5**[20,21], is not observed in the photolysis of **1** in the presence of DF (C_6D_6). Instead, its dimer **6** is formed in 25% yield[13] (Scheme 1). Dimerization of **5** has been reported to

Scheme 1. Photolytic Trapping Reaction

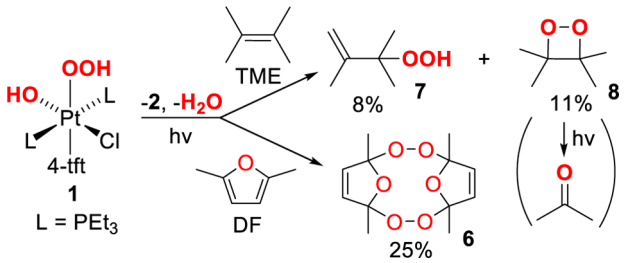

be slow at room temperature but rapid above 55−60 °C.[14] It is possible that monomer **5** is the initial product and dimerizes under the photolytic conditions. With TME (CD_2Cl_2), the expected singlet oxygen product, hydroperoxide **7**,[22,23] is observed in 8% yield[13] along with tetramethyl-1,2-dioxetane (**8**)[24] (9%) and acetone (4%) (Scheme 1). Further photolysis converts **8** to acetone,[24] indicating that acetone is likely a secondary product and that the dioxetane is actually produced in 11% yield.[13] Dioxetane **8** is not an expected product from singlet oxygen, but its formation does occur from the direct reaction of H_2O_3 with TME. This reaction has not been reported, but we found that addition of TME to a photogenerated solution of H_2O_3 at −60 °C yields **8** [see the Supporting Information (SI)].

Complex **1** is also thermally active toward elimination. Heating of a toluene-d_8 solution shows no immediate change until about 80 °C, at which point gas evolution is observed. As for the photolytic reactions, ^{31}P and ^{1}H NMR spectroscopy show the formation of **2** and water, indicating that the thermal reaction products are similar to those of the photolytic reaction (eq 1). We again tested for singlet oxygen by repeating the decomposition in the presence of TME and DF (Scheme 2). The decomposition rate is unaffected, showing that there is no direct reaction between the traps and **1**. A 15% yield[13] of dioxetane **8** is produced in the TME reaction. Again, this is not the expected product from singlet oxygen but is one of the same products of the photolytic reaction and a product of the reaction of H_2O_3 with TME (see above). Photolytic conversion of **8** to acetone was confirmed with this sample. The DF thermal reaction gives a 10% yield[13] of endoperoxide dimer **6**, which is the expected singlet oxygen product above 55−60 °C.[14] A kinetic study of the decomposition (no trap) revealed a reaction that is

Scheme 2. Thermal Trapping Reaction

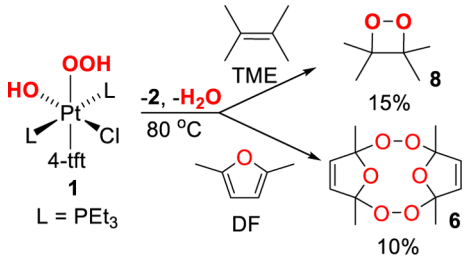

first-order in **1** with activation parameters $\Delta H^{\ddagger} = 19(1)$ kcal/mol and $\Delta S^{\ddagger} = -18(4)$ cal mol^{-1} K^{-1}.

The chemistry of **1** was modeled using density functional theory (DFT) computations with PMe_3 in place of PEt_3 (indicated with a prime on the complex numbers). An issue that immediately arises is the hydrogen bonding in **1**. While the solid-state structure of **1** is a dimer with intermolecular OOH hydrogen bonding,[1] a diffusion-ordered spectroscopy (DOSY) NMR experiment (see the SI) in acetone-d_6 indicates negligible dimer formation in solution. However, there are still options for intramolecular hydrogen bonding of the OH and OOH ligands (Figure 1). In model complex **1a′**, the OH ligand is the donor

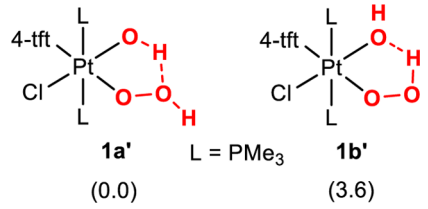

Figure 1. Intramolecular hydrogen-bonding models for **1** with calculated relative energies in kcal/mol in parentheses.

and the OOH ligand the acceptor. This is the intramolecular hydrogen-bonding pattern in the solid-state structure of **1**.[1] Complex **1b′** has the reverse pattern. Gas-phase optimization of **1a′** and **1b′** converged to minima with **1b′** at 3.6 kcal/mol higher free energy, suggesting that, at least in nonpolar, non-hydrogen-bonding solvents, the majority hydrogen-bonding structure for monomeric **1** is of type **1a′**, the same intramolecular hydrogen-bonding pattern observed in the solid-state dimer.[1]

Reductive-elimination thermodynamic values (gas phase) for **1a′** were calculated and are given in Table 1. H_2O_3 elimination is endergonic by 14.4 kcal/mol. Water and $^1O_2$($^1\Delta_g$) elimination is exergonic with $\Delta G = -11.4$ kcal/mol. Expectedly, $^3O_2$($^3\Sigma_g^-$) and water elimination is more favorable, with a calculated ΔG of −28.2 kcal/mol. The energy difference between $^1O_2$ and $^3O_2$ elimination corresponds to the O_2 singlet−triplet energy gap.

Table 1. Free Energies (DFT) for Reductive Elimination from 1a′ (Gas Phase, 25 °C, 1 atm)

products[a]	ΔG (kcal/mol)[b]
2′ + H_2O_3	14.4
2′ + H_2O + $^1O_2$ ($^1\Delta_g$)	−11.4[c]
2′ + H_2O + $^3O_2$ ($^3\Sigma_g^-$)	−28.2

[a]**2′** = *trans*-Pt(PMe_3)$_2$(Cl)(4-tft). [b]These values will be somewhat more positive in solution because of the entropy difference between solution and the gas phase.[28] [c]On the basis of the known O_2 singlet−triplet energy gap, this value is likely ∼6 kcal/mol too low (see the text).

dx.doi.org/10.1021/ja507263f | J. Am. Chem. Soc. 2014, 136, 13979−13982

Thus, our calculated gap value is 16.8 kcal/mol, which is somewhat smaller than the experimental value of 22.5 kcal/mol.[25,26] The fault likely lies with the singlet oxygen, as DFT methods are known to have difficulty with open-shell singlets.[11,27] Thus, the ΔG value of −11.4 kcal/mol for conversion of **1a′** to **2′**, H_2O, and $^1O_2$ is likely ∼6 kcal/mol too low.

As Pt(IV) complex photochemistry usually involves the lowest-energy triplet excited state, obtained either through direct excitation or through rapid (fs) internal conversion and intersystem crossing,[29,30] structures **1a′** and **1b′** were optimized as triplets. No intact structure is found for the triplet from **1b′**. Instead, optimization rapidly yields a "plateau" structure with a five-coordinate Pt−(η^1-O_2) complex and a hydrogen-bonded water molecule (Figure S21 in the SI). Further optimization gives **2′**, $^3O_2$, and H_2O, although a stationary point was not achieved.

In contrast, the triplet from **1a′** optimizes to a stationary point (37.8 kcal/mol above **1a′**) with minimum structure ^{3}**1a′** containing intact OOH and OH ligands (Figure 2). A

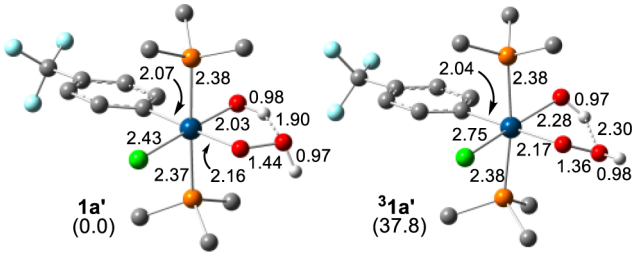

Figure 2. Optimized model structures **1a′** and ^{3}**1a′** (bond distances in Å; blue = Pt, green = Cl, orange = P, red = O, gray = C, white = H; carbon-bonded H atoms omitted). Calculated relative energies in kcal/mol are given in parentheses.

comparison of the metrical parameters of ^{3}**1a′** with those of **1a′** shows that the bonds along the Cl−Pt−OH axis have lengthened and that the O−O bond has shortened. The shorter O−O distance in ^{3}**1a′** is similar to that in the OOH radical,[31] suggesting OOH radical character in ^{3}**1a′**. This is supported by the Mulliken atom spin densities (Figure 3), which show nearly a

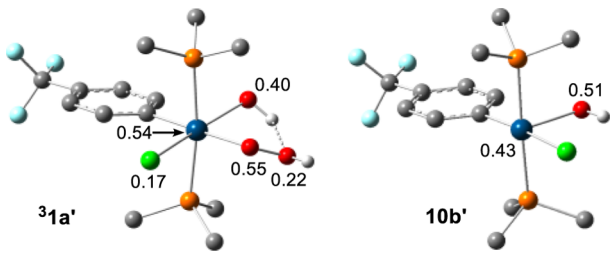

Figure 3. Mulliken atomic spin densities in ^{3}**1a′** and **10b′** (blue = Pt, green = Cl, orange = P, red = O, gray = C, white = H; carbon-bonded H atoms omitted).

full electron spin on the OOH ligand. Substantial spin density is also located on the OH ligand. Thus, ^{3}**1a′** is a likely model precursor to H_2O_3 by coupling of the radical-like OH and OOH ligands. (H_2O_3 formation from OH and OOH radical coupling in photolyzed mixtures of H_2O_2 and O_3 in an argon matrix has been proposed.[32]) Triplet ^{3}**1a′** should also be a good OOH radical donor.

The thermal reductive elimination from **1** was also examined with DFT computations. Three pathways to dioxygen, water, and **2** were considered: (1) concerted H_2O_3 reductive elimination from **1a′** or **1b′** followed by rapid H_2O_3 decomposition to singlet oxygen and water, (2) intramolecular proton transfer from the OOH ligand to the OH ligand of **1b′** to give dioxygen and water, and (3) OOH radical dissociation from **1a′** followed by abstraction of the OH ligand to form H_2O_3.

A concerted H_2O_3 reductive elimination pathway was found but can be eliminated because the transition state is prohibitively high (68.3 kcal/mol; see the SI). Relaxed potential energy scans (unrestricted) to promote proton transfer in **1b′** were conducted to probe the second pathway but failed to directly yield singlet oxygen. Instead, a scan along the O−H−OO coordinate gave η^2-O_2 complex **9′** (optimized to a stationary point) and water (Scheme 3). We have not been able to locate a transition state,

Scheme 3

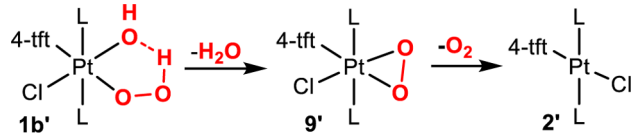

but the scan suggests a ∼25 kcal/mol barrier, consistent with the experimental free energy of activation (24 kcal/mol at 298 K). The negative entropy of activation would also be consistent with the required hydrogen-bonding interaction. Separated water and **9′** lie 15.5 kcal/mol above **1b′**. (It should be noted that **9′** is isoelectronic with known Ir(III) dioxygen complexes.[33]) A transition state for dioxygen loss from **9′** (**TS9′**; see the SI) was located 7.6 kcal/mol above **9′**, showing that formation of **9′** and water would be rate-limiting.

Thermolysis of the Pt−OOH bond of **1a′** was evaluated by calculating the energy difference between **1a′** and OOH radical + doublet Pt(PMe_3)$_2$(Cl)(OH)(4-tft) (**10′**). (Cl or OH radical loss is higher in energy.) Geometry optimization of **10′** yielded three square-pyramidal isomers with an axial Cl ligand (**10a′**), an axial OH ligand (**10b′**), and an axial 4-tft ligand (**10c′**). The lowest-energy isomer is **10b′** (4.1 kcal/mol below **10a′** and 11.7 kcal/mol below **10c′**), and with an OOH radical it lies only 22.8 kcal/mol above **1a′**, making Pt−OOH bond homolysis a viable first step in the thermal decomposition (Scheme 4). Coupled

Scheme 4

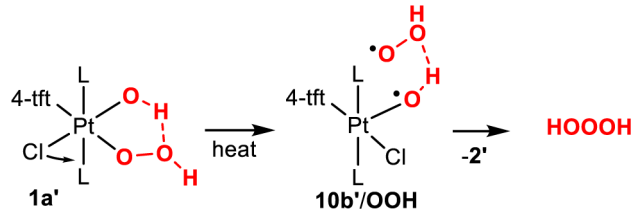

isomerization with Pt−OOH bond breaking could account for the experimental negative activation entropy. Additionally, the spin density in **10b′** is strongly localized on the OH ligand (Figure 3), suggesting facile OH abstraction by the OOH radical and formation of H_2O_3. Crossing of the singlet thermal pathway and the photochemical triplet pathway to H_2O_3 may occur at this point.

Finally, it should be noted that thermal access to the triplet is possible, although triplet ^{3}**1a′** is calculated to be nearly 40 kcal/mol above singlet **1a′**. If the analogous triplet for **1** is situated at a similar energy relative to **1**, then thermal access to the triplet

dx.doi.org/10.1021/ja507263f | J. Am. Chem. Soc. 2014, 136, 13979−13982

would not be consistent with the activation parameters for the thermal elimination.

In conclusion, hydroperoxo-hydroxo complex **1** has been found to photoreductively eliminate H_2O_3 in ~20% yield at −60 °C. DFT results suggest that the photoreaction occurs through a triplet excited state (modeled using ^{3}**1a**′) with high OOH and OH radical character, leading to coupling of OH and OOH. (H_2O_2 and acetone peroxides **3** and **4**, also formed in acetone-d_6, may be produced by "leakage" of OOH radicals from the excited state or, in the case of **3** and **4**, by direct reaction of acetone with the excited state.) The DFT results also suggest that the photolysis products may depend on the intramolecular hydrogen-bonding state of **1**, with the lowest-energy state yielding the H_2O_3 products and a slightly higher state giving water and dioxygen. Thermolysis and room-temperature photolysis of **1** give water and dioxygen as final products, but in both cases trapping experiments with DF and TME give results generally consistent with initial formation of H_2O_3. The low yield of singlet oxygen trapping product **7** observed with TME in the room-temperature photolysis may result from partial decomposition of H_2O_3 to singlet oxygen and water prior to reaction with TME. Singlet oxygen emission experiments should provide information on the involvement of singlet oxygen in these reactions.[26] On the basis of the above results and our previous results[1,12,19] with analogous complexes, the *trans*-Pt(IV)L_2(R)X_3 system is proving to be a versatile platform for elimination chemistry. Other complexes that should eliminate unusual molecules are currently under investigation.

■ ASSOCIATED CONTENT

Supporting Information

Experimental procedures, NMR data, kinetic data, and DFT coordinates and energies. This material is available free of charge via the Internet at http://pubs.acs.org.

■ AUTHOR INFORMATION

Corresponding Author

sharpp@missouri.edu

Author Contributions

The authors contributed equally.

Notes

The authors declare no competing financial interest.

■ ACKNOWLEDGMENTS

Support was provided by the U.S. Department of Energy, Office of Basic Energy Sciences (DE-FG02-88ER13880). We thank Dr. Wei Wycoff for assistance with the NMR measurements. Computations were performed on the HPC resources at the University of Missouri Bioinformatics Consortium (UMBC).

■ REFERENCES

(1) Wickramasinghe, L. A.; Sharp, P. R. *Inorg. Chem.* **2014**, *53*, 1430.
(2) Becht, A.; Vogler, A. *Inorg. Chem.* **1993**, *32*, 2835.
(3) Knor, G.; Vogler, A.; Roffia, S.; Paolucci, F.; Balzani, V. *Chem. Commun.* **1996**, 1643.
(4) Kohl, S. W.; Weiner, L.; Schwartsburd, L.; Konstantinovski, L.; Shimon, L. J. W.; Ben-David, Y.; Iron, M. A.; Milstein, D. *Science* **2009**, *324*, 74.
(5) Vogler, A.; Kunkely, H. *Inorg. Chem. Commun.* **2011**, *14*, 96.
(6) Petruzzella, E.; Margiotta, N.; Ravera, M.; Natile, G. *Inorg. Chem.* **2013**, *52*, 2393.
(7) Cerkovnik, J.; Plesničar, B. *J. Am. Chem. Soc.* **1993**, *115*, 12169.
(8) Cerkovnik, J.; Plesničar, B. *Chem. Rev.* **2013**, *113*, 7930.
(9) Nyffeler, P. T.; Boyle, N. A.; Eltepu, L.; Wong, C.-H.; Eschenmoser, A.; Lerner, R. A.; Wentworth, P. *Angew. Chem., Int. Ed.* **2004**, *43*, 4656.
(10) Wentworth, P., Jr.; Jones, L. H.; Wentworth, A. D.; Zhu, X.; Larsen, N. A.; Wilson, I. A.; Xu, X.; Goddard, W. A., III; Janda, K. D.; Eschenmoser, A.; Lerner, R. A. *Science* **2001**, *293*, 1806.
(11) Xu, X.; Muller, R. P.; Goddard, W. A., III. *Proc. Natl. Acad. Sci. U.S.A.* **2002**, *99*, 3376.
(12) Karikachery, A. R.; Lee, H. B.; Masjedi, M.; Ross, A.; Moody, M. A.; Cai, X.; Chui, M.; Hoff, C.; Sharp, P. R. *Inorg. Chem.* **2013**, *52*, 4113.
(13) % yield = 100% × (moles of product/moles of **1**).
(14) Paulsen, P. J.; Cooke, W. D. *Anal. Chem.* **1963**, *35*, 1560.
(15) Cambridge Isotope Laboratories, I.; Cambridge Isotope Laboratories: Tewksbury, MA, 2014; Vol. *2014*, https://www.isotope.com/userfiles/files/assetLibrary/NMR_solvents_data_chart_&_storage.pdf .
(16) Rieche, A. *Angew. Chem.* **1958**, *70*, 251.
(17) Milas, N. A.; Golubovic, A. *J. Am. Chem. Soc.* **1959**, *81*, 6461.
(18) Sashidhara, K. V.; Avula, S. R.; Ravithej Singh, L.; Palnati, G. R. *Tetrahedron Lett.* **2012**, *53*, 4880.
(19) Perera, T. A.; Masjedi, M.; Sharp, P. R. *Inorg. Chem.* **2014**, *53*, 7608.
(20) Gollnick, K.; Griesbeck, A. *Angew. Chem.* **1983**, *95*, 751.
(21) Kuo, Y.-H.; Shih, K.-S.; Lee, G.-H.; Wang, Y. *Heterocycles* **1988**, *27*, 599.
(22) Foote, C. S. *Acc. Chem. Res.* **1968**, *1*, 104.
(23) Clennan, E. L. *Tetrahedron* **2000**, *56*, 9151.
(24) Kotani, H.; Ohkubo, K.; Fukuzumi, S. *J. Am. Chem. Soc.* **2004**, *126*, 15999.
(25) Herzberg, G. *Spectra of Diatomic Molecules*; Van Nostrand Reinhold: New York, 1950.
(26) Schweitzer, C.; Schmidt, R. *Chem. Rev.* **2003**, *103*, 1685.
(27) Cramer, C. J. *Essentials of Computational Chemistry: Theories and Models*, 2nd ed.; John Wiley & Sons: Chichester, U.K., 2004.
(28) Martin, R. L.; Hay, P. J.; Pratt, L. R. *J. Phys. Chem. A* **1998**, *102*, 3565.
(29) Glebov, E. M.; Kolomeets, A. V.; Pozdnyakov, I. P.; Plyusnin, V. F.; Grivin, V. P.; Tkachenko, N. V.; Lemmetyinen, H. *RSC Adv.* **2012**, *2*, 5768.
(30) Zheldakov, I. L.; Ryazantsev, M. N.; Tarnovsky, A. N. *J. Phys. Chem. Lett.* **2011**, *2*, 1540.
(31) Parreira, R. L. T.; Galembeck, S. E. *J. Am. Chem. Soc.* **2003**, *125*, 15614.
(32) Xu, X.; Goddard, W. A., III. *Proc. Natl. Acad. Sci. U.S.A.* **2002**, *99*, 15308.
(33) Lawson, H. J.; Atwood, J. D. *J. Am. Chem. Soc.* **1989**, *111*, 6223.